



Resonance $X(7300)$: excited $2S$ tetraquark or hadronic molecule $\chi_{c1}\chi_{c1}$?

S. S. Agaev¹, K. Azizi^{2,3,a}, B. Barsbay⁴, H. Sundu⁵

¹ Institute for Physical Problems, Baku State University, 1148 Baku, Azerbaijan

² Department of Physics, University of Tehran, North Karegar Avenue, Tehran 14395-547, Iran

³ Department of Physics, Doğuş University, Dudullu-Ümraniye, 34775 Istanbul, Turkey

⁴ Division of Optometry, School of Medical Services and Techniques, Doğuş University, 34775 Istanbul, Turkey

⁵ Department of Physics Engineering, Istanbul Medeniyet University, 34700 Istanbul, Turkey

Received: 14 September 2023 / Accepted: 13 October 2023 / Published online: 3 November 2023
© The Author(s) 2023

Abstract We explore the first radial excitation X_{4c}^* of the fully charmed diquark-antidiquark state $X_{4c} = cc\bar{c}\bar{c}$ built of axial-vector components, and the hadronic molecule $\mathcal{M} = \chi_{c1}\chi_{c1}$. The masses and current couplings of these scalar states are calculated in the context of the QCD two-point sum rule approach. The full widths of X_{4c}^* and \mathcal{M} are evaluated by taking into account their kinematically allowed decay channels. We find partial widths of these processes using the strong couplings g_i^* and $G_i^{(*)}$ at the $X_{4c}^*(\mathcal{M})$ -conventional mesons vertices computed by means of the QCD three-point sum rule method. The predictions obtained for the parameters $m = (7235 \pm 75)$ MeV, $\Gamma = (144 \pm 18)$ MeV and $\tilde{m} = (7180 \pm 120)$ MeV, $\tilde{\Gamma} = (169 \pm 21)$ MeV of these structures, are compared with the experimental data of the CMS and ATLAS Collaborations. In accordance to these results, within existing errors of measurements and uncertainties of the theoretical calculations, both the excited tetraquark and hadronic molecule may be considered as candidates to the resonance $X(7300)$. Detailed analysis, however, demonstrates that the preferable model for $X(7300)$ is an admixture of the molecule \mathcal{M} and sizeable part of X_{4c}^* .

1 Introduction

The multi-quark hadrons composed of exclusively heavy quarks were in agenda of researches from first years of the parton model and QCD. During past decades much was done to investigate features of such particles, calculate their parameters in the context of different models, study production and decay mechanisms of these hadrons. Reports of the LHCb,

ATLAS and CMS Collaborations on X resonances in the 6.2–7.3 GeV mass range became one of important experimental achievements in the physics of fully charmed four-quark mesons [1–3]. The structures $X(6200)$, $X(6600)$, $X(6900)$ and $X(7300)$ observed by these experiments in the di- J/ψ and $J/\psi\psi'$ mass distributions provide useful information and allow one to compare numerous theoretical predictions with the masses and widths of these states.

These discoveries generated new theoretical activities to explain observed states, reveal their internal structures [4–16]. The fully heavy X resonances were considered as scalar four-quark mesons with diquark-antidiquark or hadronic molecule organizations [4–8]. For example, the resonance $X(6900)$ may be a diquark-antidiquark state with pseudoscalar ingredients, or hadronic molecule $\chi_{c0}\chi_{c0}$ [5]. The structure $X(6200)$ was interpreted as a ground-level tetraquark with the spin-parities $J^{PC} = 0^{++}$ or 1^{+-} , whereas $X(6600)$ – as its first radial excitation [6]. The four structures $X(6200) - X(7300)$ were assigned to be different excited tetraquark states [7, 8].

Alternative scenarios explain appearance of the X resonances by coupled-channel effects. Thus, using this approach the authors of Ref. [11] predicted existence of the near-threshold state $X(6200)$ with $J^{PC} = 0^{++}$ or 2^{++} in the di- J/ψ system. Coupled-channel effects may also generate a pole structure identified in Ref. [13] with $X(6900)$, and lead to emergence of a bound state $X(6200)$, and resonances $X(6680)$ and $X(7200)$, which can be classified as broad and narrow structures, respectively.

Production mechanisms of fully heavy tetraquarks in different processes became topics for interesting investigations [17, 18]. Thus, inclusive production of fully charmed S -wave four-quark mesons at the LHC energies was studied in the

^a e-mail: kazem.azizi@ut.ac.ir (corresponding author)

nonrelativistic QCD factorization framework in Ref. [17]. Production of fully-heavy tetraquark states in pp and pA collisions through the double parton scattering mechanism was considered in Ref. [18], in which it was shown that a search for such states is feasible in the future runs of LHC and in Future Circular Collider.

The fully heavy four-quark mesons were studied also in our articles [19–21]. The scalar tetraquarks $X_{4c} = cc\bar{c}\bar{c}$ and $X_{4b} = bb\bar{b}\bar{b}$ built of axial-vector diquarks were explored in Ref. [19]. It was demonstrated that X_{4c} with the mass (6570 ± 55) MeV and full width (110 ± 21) MeV is nice candidate to the resonance $X(6600)$. The fully beauty state X_{4b} has the mass (18540 ± 50) MeV that is smaller than the $\eta_b\eta_b$ threshold therefore it cannot be seen in $\eta_b\eta_b$ or $\Upsilon(1S)\Upsilon(1S)$ mass distributions. The X_{4b} can decay to open-beauty mesons through $\bar{b}b$ annihilation to gluon(s) that triggers $X_{4b} \rightarrow B^+B^-$ and other decays [9]. Electromagnetic decays to photons and leptons are alternative channels for transformation of X_{4b} to conventional particles.

The scalar tetraquarks T_{4c} and T_{4b} composed of pseudoscalar diquarks were explored in Ref. [20], in which we computed their masses and widths. The parameters $m = (6928 \pm 50)$ MeV and $\tilde{\Gamma}_{4c} = (128 \pm 22)$ MeV of T_{4c} are in excellent agreements with relevant CMS data, therefore we interpreted it as the resonance $X(6900)$. The exotic meson T_{4b} decays to $\eta_b\eta_b$ pairs and can be detected in the mass distribution of these mesons. It is interesting that the hadronic molecule $\chi_{c0}\chi_{c0}$ (a brief form of $\chi_{c0}(1P)\chi_{c0}(1P)$) has similar parameters and is another candidate to $X(6900)$ [21]. Hence, $X(6900)$ may be considered as a linear superposition of the molecule $\chi_{c0}\chi_{c0}$ and diquark-antidiquark state T_{4c} .

The lowest lying structure among X states is the resonance $X(6200)$, that may be interpreted as the molecule $\eta_c\eta_c$. In fact, the mass (6264 ± 50) MeV and full width (320 ± 72) MeV of the molecule $\eta_c\eta_c$ agree with the LHCb-ATLAS-CMS data [21].

The last position in the list of new X structures is held by the resonance $X(7300)$. This state was detected in both the di- J/ψ and $J/\psi\psi'$ mass distributions. In Ref. [19], we used this fact to make assumptions about its nature, and argued that $X(7300)$ maybe is the $2S$ radial excitation of the exotic meson $X(6600)$. Another option for $X(7300)$ is the hadronic molecule model $\chi_{c1}(1P)\chi_{c1}(1P)$ (in what follows $\chi_{c1}\chi_{c1}$) that may have close parameters.

In the present article, we address problems connected with the resonance $X(7300)$ in attempts to describe its parameters in the four-quark model. To this end, we calculate the mass and width of the first radial excitation X_{4c}^* of the diquark-antidiquark state X_{4c} . The full width of X_{4c}^* is evaluated using its kinematically allowed decays to $J/\psi J/\psi$, $J/\psi\psi'$, $\eta_c\eta_c$, $\eta_c\eta_c(2S)$, $\eta_c\chi_{c1}$, $\chi_{c0}\chi_{c0}$, and $\chi_{c1}\chi_{c1}$ mesons. We are also going to perform the similar analysis in the case of the molecule $\mathcal{M} = \chi_{c1}\chi_{c1}$. We will compare predictions for

parameters of X_{4c}^* and \mathcal{M} with experimental data, and each other to make decision about the nature of $X(7300)$.

This article is organized in the following form: In Sect. 2, we explore the excited tetraquark X_{4c}^* and compute its mass and full width. The same analysis for the molecule \mathcal{M} is carried out in Sect. 3. In the last Sect. 4, we present our brief conclusions. Appendix contains the heavy quark propagator and some of correlation functions used in the present analysis.

2 Radially excited state X_{4c}^*

In this section, we explore the first radial excitation X_{4c}^* of the scalar tetraquark X_{4c} built of axial-vector diquarks. The mass and current coupling of this state are computed by means of the QCD two-point sum rule (SR) approach [22,23]. To evaluate partial widths of the kinematically allowed decay channels of X_{4c}^* , we are going to employ the three-point sum rule method, which is necessary to find strong couplings at corresponding three-particle vertices. It is worth noting that the SR methods are powerful nonperturbative tools to study conventional hadrons, but they can also be applied for analyses of multi-quark particles [24–26].

2.1 Mass m and coupling f of X_{4c}^*

The sum rules for the mass m and current coupling f of the tetraquark X_{4c}^* can be extracted from analysis of the correlation function

$$\Pi(p) = i \int d^4x e^{ipx} \langle 0 | \mathcal{T} \{ J(x) J^\dagger(0) \} | 0 \rangle, \quad (1)$$

where \mathcal{T} is the time-ordered product of two currents, and $J(x)$ is the interpolating current for the states X_{4c} and X_{4c}^* .

We model X_{4c} and X_{4c}^* as tetraquarks built of the axial-vector diquark $c^T C \gamma_\mu c$ and axial-vector antidiquark $\bar{c} \gamma_\mu C \bar{c}^T$. Then, the interpolating current is determined by the expression

$$J(x) = c_a^T(x) C \gamma_\mu c_b(x) \bar{c}_a(x) \gamma^\mu C \bar{c}_b^T(x), \quad (2)$$

with a and b being color indices. In Eq. (2) $c(x)$ is c -quark fields, and C is the charge conjugation matrix. The current $J(x)$ describes the diquark-antidiquark states with spin-parities $J^{PC} = 0^{++}$.

The ground-level particle with this quark content and quantum numbers is the tetraquark X_{4c} which was investigated in our paper [19]. We computed its mass m_0 and coupling f_0 by employing the two-point SR approach. We took into account explicitly only the ground-state term and included all other contributions to a class of “higher resonances and continuum states”. We refer to this standard treatment as “ground-state+continuum” approximation.

To derive sum rules for m and f , we express the correlation function $\Pi(p)$ in terms of X_{4c} and X_{4c}^* tetraquarks' masses and couplings. Having inserted a complete set of intermediate states with the same content and quantum numbers of these tetraquarks, and carried out integration over x , we get

$$\begin{aligned} \Pi^{\text{Phys}}(p) = & \frac{\langle 0|J|X_{4c}(p)\rangle\langle X_{4c}(p)|J^\dagger|0\rangle}{m_0^2 - p^2} \\ & + \frac{\langle 0|J|X_{4c}^*(p)\rangle\langle X_{4c}^*(p)|J^\dagger|0\rangle}{m^2 - p^2} \dots \end{aligned} \tag{3}$$

This expression contains two terms corresponding to the ground-state particle X_{4c} with the mass m_0 and a contribution coming from the first radially excited state, i.e., from $2S$ level tetraquark X_{4c}^* . Here, the ellipses stand for the effects of higher resonances and continuum states. This approach is “ground-level+first excited state +continuum” approximation.

The $\Pi^{\text{Phys}}(p)$ can be simplified using the matrix elements

$$\langle 0|J|X_{4c}(p)\rangle = f_0 m_0, \quad \langle 0|J|X_{4c}^*(p)\rangle = f m, \tag{4}$$

where f_0 and f are current couplings of the X_{4c} and X_{4c}^* , respectively. Then, we get

$$\Pi^{\text{Phys}}(p) = \frac{f_0^2 m_0^2}{m_0^2 - p^2} + \frac{f^2 m^2}{m^2 - p^2} + \dots \tag{5}$$

This function contains only the Lorentz structure proportional to I , hence the invariant amplitude $\Pi^{\text{Phys}}(p^2)$ necessary for our analysis is defined by rhs of Eq. (5).

The QCD side of the sum rules is formed by the correlation function $\Pi(p)$ expressed using c -quark propagators and calculated in the operator product expansion (OPE) with some accuracy. In the case under discussion, $\Pi^{\text{OPE}}(p)$ and corresponding amplitude $\Pi^{\text{OPE}}(p^2)$ were computed in Ref. [19]. There, we also found the parameters m_0 and f_0 of the ground-state particle X_{4c} , which appear in the present analysis as input quantities.

After the Borel transformation and continuum subtraction the SR equality takes the form

$$f^2 m^2 e^{-m^2/M^2} = \Pi(M^2, s_0) - f_0^2 m_0^2 e^{-m_0^2/M^2}, \tag{6}$$

which in conjunction with the derivation of Eq. (6) over $d/d(-1/M^2)$, can be utilized to find sum rules for m and f . Here, $\Pi(M^2, s_0)$ is the amplitude $\Pi^{\text{OPE}}(p^2)$ after the Borel transformation and subtraction operations, and M^2 and s_0 are corresponding parameters.

The $\Pi(M^2, s_0)$ is given by the formula

$$\Pi(M^2, s_0) = \int_{16m_c^2}^{s_0} ds \rho^{\text{OPE}}(s) e^{-s/M^2}. \tag{7}$$

where $\rho^{\text{OPE}}(s)$ is a two-point spectral density. It consists of the perturbative contribution $\rho^{\text{pert.}}(s)$ and the dimension-4 nonperturbative term $\sim \langle \alpha_s G^2/\pi \rangle$: The explicit expression of $\rho^{\text{pert.}}(s)$ can be found in Ref. [19].

To carry out numerical computations, one needs the gluon vacuum condensate $\langle \alpha_s G^2/\pi \rangle = (0.012 \pm 0.004) \text{ GeV}^4$ and c -quark mass $m_c = (1.27 \pm 0.02) \text{ GeV}$. A crucial problem to be clarified is a choice of the parameters M^2 and s_0 . The regions in which they can be changed should meet known restrictions of SR computations. Stated differently, M^2 and s_0 have to be fixed in such a way that to ensure dominance of the pole contribution (PC) and perturbative term over a nonperturbative one. The convergence of OPE and a stability of extracted observables against variations of the Borel parameter M^2 are also among important constraints. Because, $\Pi(M^2, s_0)$ does not contain quark and mixed condensates the dominance of PC and stability of extracted quantities play key role in choosing parameters M^2 and s_0 .

In the first phase of computations, we fix the regions for M^2 and s_0 in order to activate in Eq. (3) only the ground-state term. This task was fulfilled in Ref. [19], where M^2 and s_0 were varied inside the regions

$$M^2 \in [5.5, 7] \text{ GeV}^2, \quad s_0 \in [49, 50] \text{ GeV}^2. \tag{8}$$

As a result, we evaluated the mass m_0 and coupling f_0 of the ground-state tetraquark X_{4c}

$$\begin{aligned} m_0 &= (6570 \pm 55) \text{ MeV}, \\ f_0 &= (5.61 \pm 0.39) \times 10^{-2} \text{ GeV}^4. \end{aligned} \tag{9}$$

At the second stage of studies, we use m_0 and f_0 in Eq. (6) as input parameters and calculate the mass m and coupling f of the excited state

$$\begin{aligned} m &= (7235 \pm 75) \text{ MeV}, \\ f &= (8.0 \pm 0.9) \times 10^{-2} \text{ GeV}^4. \end{aligned} \tag{10}$$

To compute Eq. (10), we use the working regions

$$M^2 \in [5.5, 7] \text{ GeV}^2, \quad s_0^* \in [55, 56] \text{ GeV}^2, \tag{11}$$

which obey all constraints imposed on $\Pi(M^2, s_0)$ by the SR analysis. In fact, the pole contribution changes inside limits $0.93 \geq \text{PC} \geq 0.71$, at the minimum of $M^2 = 5.5 \text{ GeV}^2$ the nonperturbative term is negative and constitutes only 1.4% part of the correlation function. The extracted quantities m and coupling f bear residual dependence on the parameters M^2 and s_0^* which is a main source of theoretical uncertainties. These effects are equal to $\pm 1\%$ in the case of m , and to $\pm 11\%$ for f staying within limits acceptable for the SR computations. The behavior of the mass m under variations of M^2 and s_0^* is shown in Fig. 1.

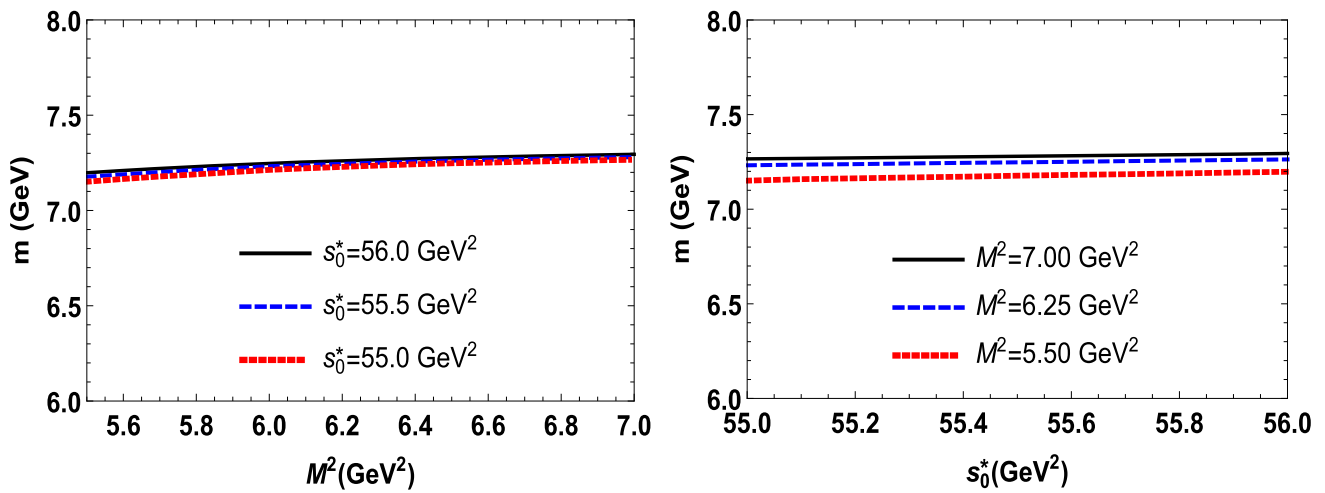


Fig. 1 Mass of the tetraquark X_{4c}^* as a function of the Borel M^2 (left), and the continuum threshold s_0^* parameters (right)

Because we consider two terms in Eq. (5), and find parameters of the ground-level and radially excited tetraquarks, there is a necessity to check a self-consistency of performed studies. Indeed, the parameters s_0 and s_0^* separate contributions of interest from ones which are modeled using the assumption about quark-hadron duality. Therefore, in these studies the inequalities $m_0^2 < s_0$ and $s_0 < m^2 < s_0^*$ should be satisfied: With results of the numerical analysis at hand, it is not difficult to verify these relations.

The prediction for the mass $m = 7235$ MeV of the $2S$ excited tetraquark X_{4c}^* within uncertainties of calculations and errors of experiments is consistent with values $m^{\text{ATL}} = 7220 \pm 30^{+20}_{-30}$ MeV and $m^{\text{CMS}} = 7287^{+20}_{-18} \pm 5$ MeV, respectively. In our article [19] we supposed that the resonance $X(7300)$ is $2S$ excited state of $X(6600)$. This assumption based on the fact that the ATLAS Collaboration detected the resonances $X(6600)$ and $X(7300)$ in $J/\psi J/\psi$ and $J/\psi \psi'$ mass distributions, respectively. Because the mass difference between mesons ψ' and J/ψ is around 590 MeV, and a comparable mass splitting (600 – 735) MeV exists in the $X(7300) - X(6600)$ system, it is natural to assume that $X(7300)$ is excitation of $X(6600)$. Our results for the masses of X_{4c} and X_{4c}^* differ by amount 665 MeV and seem support this scenario.

2.2 The full width of X_{4c}^*

The mass m of the excited tetraquark X_{4c}^* allow us to determine its decay channels, and evaluate full width of this state. It is clear, that decays to $J/\psi J/\psi$, $J/\psi \psi'$, $\eta_c \eta_c$, $\eta_c \eta_c(2S)$, $\eta_c \chi_{c1}$, $\chi_{c0} \chi_{c0}$, and $\chi_{c1} \chi_{c1}$ mesons are among such allowed channels. It is worth noting that decay $X_{4c}^* \rightarrow \eta_c \chi_{c1}$ is the P -wave process, whereas the remaining ones are S -wave decays.

We are going to explain in a detailed form only processes $X_{4c}^* \rightarrow J/\psi J/\psi$ and $X_{4c}^* \rightarrow J/\psi \psi'$, and provide final results for other channels. The partial widths of these decays are governed by the strong couplings g_i^* at the vertices $X_{4c}^* J/\psi J/\psi$, and $X_{4c}^* J/\psi \psi'$. These couplings can be evaluated using the following three-point correlation function

$$\Pi_{\mu\nu}(p, p') = i^2 \int d^4x d^4y e^{ip'y} e^{-ipx} \langle 0 | T \{ J_\mu^\psi(y) \times J_\nu^\psi(0) J^\dagger(x) \} | 0 \rangle, \tag{12}$$

where $J_\mu^\psi(x)$ is the interpolating current for the mesons J/ψ and ψ'

$$J_\mu^\psi(x) = \bar{c}_i(x) \gamma_\mu c_i(x), \tag{13}$$

with $i = 1, 2, 3$ being the color indices.

We apply usual recipes of the sum rule method and express the correlation function $\Pi_{\mu\nu}(p, p')$ in terms of physical parameters of particles. Because the tetraquark X_{4c}^* decays both to $J/\psi J/\psi$ and $J/\psi \psi'$ pairs, we isolate in $\Pi_{\mu\nu}(p, p')$ contributions of the mesons J/ψ and ψ' from ones of higher resonances and continuum states. But the current $J(x)$ also couples to the ground-state tetraquark X_{4c} . Therefore, for the physical side of the sum rule $\Pi_{\mu\nu}^{\text{Phys}}(p, p')$, we get

$$\begin{aligned} \Pi_{\mu\nu}^{\text{Phys}}(p, p') = & \sum_{i=1,2} \frac{\langle 0 | J_\mu^\psi | J/\psi(p') \rangle \langle 0 | J_\nu^\psi | J/\psi(q) \rangle}{p^2 - m_J^2} \frac{1}{q^2 - m_J^2} \\ & \times \langle J/\psi(p') J/\psi(q) | X_{4c}^I(p) \rangle \frac{\langle X_{4c}^I(p) | J^\dagger | 0 \rangle}{p^2 - m_I^2} \\ & + \sum_{i=1,2} \frac{\langle 0 | J_\mu^\psi | \psi(p') \rangle \langle 0 | J_\nu^\psi | J/\psi(q) \rangle}{p^2 - m_{\psi'}^2} \frac{1}{q^2 - m_J^2} \end{aligned}$$

$$\times \langle \psi(p') J / \psi(q) | X_{4c}^I(p) \rangle \frac{\langle X_{4c}^I(p) | J^\dagger | 0 \rangle}{p^2 - m_I^2} \dots, \tag{14}$$

where $m_J = (3096.900 \pm 0.006)$ MeV and $m_\psi = (3686.10 \pm 0.06)$ MeV are the masses of J/ψ and ψ' mesons [27]. To write down $\Pi_{\mu\nu}^{\text{Phys}}(p, p')$ in a compact form, we use in Eq. (14) notations $X_{4c}^1 = X_{4c}$, $X_{4c}^2 = X_{4c}^*$ and $m_1^2 = m_0^2$, $m_2^2 = m^2$.

The function $\Pi_{\mu\nu}^{\text{Phys}}(p, p')$ can be expressed in terms of mesons and tetraquarks masses and decay constants (couplings). To this end, one should use the matrix elements of the tetraquarks Eq. (4), as well as the matrix elements

$$\begin{aligned} \langle 0 | J_\mu^\psi | J/\psi(p) \rangle &= f_J m_J \varepsilon_\mu(p), \\ \langle 0 | J_\mu^\psi | \psi'(p) \rangle &= f_\psi m_\psi \tilde{\varepsilon}_\mu(p), \end{aligned} \tag{15}$$

and

$$\begin{aligned} \langle J/\psi(p') J/\psi(q) | X_{4c}(p) \rangle &= g_1(q^2) [q \cdot p' \varepsilon^*(p') \cdot \varepsilon^*(q) \\ &\quad - q \cdot \varepsilon^*(p') p' \cdot \varepsilon^*(q)], \\ \langle \psi(p') J/\psi(q) | X_{4c}(p) \rangle &= g_2(q^2) [q \cdot p' \tilde{\varepsilon}^*(p') \cdot \varepsilon^*(q) \\ &\quad - q \cdot \tilde{\varepsilon}^*(p') p' \cdot \varepsilon^*(q)]. \end{aligned} \tag{16}$$

Here, $f_J = (409 \pm 15)$ MeV, $f_\psi = (279 \pm 8)$ MeV and $\varepsilon_\mu, \tilde{\varepsilon}_\mu$ are the decay constants and polarization vectors of the mesons J/ψ and ψ' [27, 28], respectively. In the vertices with the excited tetraquark $X_{4c}^*(p)$ one should write form factors $g_1^*(q^2)$ and $g_2^*(q^2)$.

Having used these matrix elements and carried out simple calculations, we find for $\Pi_{\mu\nu}^{\text{Phys}}(p, p')$

$$\begin{aligned} \Pi_{\mu\nu}^{\text{Phys}}(p, p') &= g_1(q^2) f_0 m_0 f_J^2 m_J^2 F_{\mu\nu}(m_0, m_J) \\ &\quad + g_1^*(q^2) f m f_J^2 m_J^2 F_{\mu\nu}(m, m_J) \\ &\quad + g_2(q^2) f_0 m_0 f_J m_J f_\psi m_\psi F_{\mu\nu}(m_0, m_\psi) \\ &\quad + g_2^*(q^2) f m f_J m_J f_\psi m_\psi F_{\mu\nu}(m, m_\psi) + \dots, \end{aligned} \tag{17}$$

where

$$F_{\mu\nu}(a, b) = \frac{[(a^2 - b^2 - q^2) g_{\mu\nu} - 2q_\mu p'_\nu]}{2(p^2 - a^2)(p'^2 - b^2)(q^2 - m_J^2)}. \tag{18}$$

As is seen, there are two structures in $\Pi_{\mu\nu}^{\text{Phys}}(p, p')$ which can be used for SR analysis. To derive the sum rules for the form factors $g_i^{(*)}(q^2)$, we work with the Lorentz structure $g_{\mu\nu}$, and corresponding invariant amplitude $\Pi^{\text{Phys}}(p^2, p'^2, q^2)$.

After the double Borel transformation of the function $\Pi^{\text{Phys}}(p^2, p'^2, q^2)$ over the variables $-p^2$ and $-p'^2$, we get

$$\begin{aligned} \mathcal{B}\Pi^{\text{Phys}}(p^2, p'^2, q^2) &= g_1(q^2) f_0 m_0 f_J^2 m_J^2 F(m_0, m_J) \\ &\quad + g_1^*(q^2) f m f_J^2 m_J^2 F(m, m_J) \\ &\quad + g_2(q^2) f_0 m_0 f_J m_J f_\psi m_\psi F(m_0, m_\psi) \\ &\quad + g_2^*(q^2) f m f_J m_J f_\psi m_\psi F(m, m_\psi) + \dots, \end{aligned} \tag{19}$$

with $F(a, b)$ being equal to

$$F(a, b) = \frac{(a^2 - b^2 - q^2)}{2(q^2 - m_J^2)} e^{-a^2/M_1^2} e^{-b^2/M_2^2}. \tag{20}$$

The second component of the sum rules is the same correlation function $\Pi_{\mu\nu}^{\text{OPE}}(p, p')$, but calculated using the c -quark propagators. The function $\Pi_{\mu\nu}^{\text{OPE}}(p, p')$ and invariant amplitude $\Pi^{\text{OPE}}(p^2, p'^2, q^2)$ were computed in Ref. [19]. Having equated $\mathcal{B}\Pi^{\text{Phys}}(p^2, p'^2, q^2)$ and the doubly Borel transformation of the amplitude $\Pi^{\text{OPE}}(p^2, p'^2, q^2)$, and performed the continuum subtractions, we find the sum rule equality, right-hand side of which is determined by the function

$$\begin{aligned} \Pi(\mathbf{M}^2, \mathbf{s}_0, q^2) &= \int_{16m_c^2}^{s_0} ds \int_{4m_c^2}^{s'_0} ds' \rho(s, s', q^2) \\ &\quad \times e^{-s/M_1^2} e^{-s'/M_2^2}. \end{aligned} \tag{21}$$

where $\mathbf{M}^2 = (M_1^2, M_2^2)$ and $\mathbf{s}_0 = (s_0, s'_0)$ are the Borel and continuum threshold parameters, respectively. A spectral density $\rho(s, s', q^2)$ is found as an imaginary part of $\Pi^{\text{OPE}}(p^2, p'^2, q^2)$. Let us note that parameters (M_1^2, \mathbf{s}_0) and (M_2^2, s'_0) correspond to $X_{4c} - X_{4c}^*$ and $J/\psi - \psi'$ channels, respectively.

The equality Eq. (19) obtained by this way contains four unknown form factors $g_{1(2)}^{(*)}(q^2)$. One of possible methods to extract them from this equality is to calculate its derivatives over $-1/M_1^2$ and $-1/M_2^2$. But then final expressions for $g_{1(2)}^{(*)}(q^2)$ become rather complicated, which may reduce an accuracy of numerical analyses. Here, we pursue the alternative policy: By choosing appropriate subtraction parameters in $X_{4c} - X_{4c}^*$ and $J/\psi - \psi'$ channels, we include in analysis terms from Eq. (19) one by one. These operations change number of components in $\mathcal{B}\Pi^{\text{Phys}}$ and integration limits in $\Pi(\mathbf{M}^2, \mathbf{s}_0, q^2)$. At each new stage, we take into account results obtained in previous steps, and solve subsequent equations with only one unknown form factor.

First of all, let us note that the form factor $g_1(q^2)$ was evaluated in Ref. [19]. It corresponds to the vertex $X_{4c} J/\psi J/\psi$ and is necessary to compute the partial width of the decay $X_{4c} \rightarrow J/\psi J/\psi$. To calculate $g_1(q^2)$, we fixed parameters (M_1^2, \mathbf{s}_0) as in Eq. (8), whereas for (M_2^2, s'_0) used

$$M_2^2 \in [4, 5] \text{ GeV}^2, s'_0 \in [12, 13] \text{ GeV}^2, \tag{22}$$

where s'_0 is limited by the mass m_ψ^2 of the next state in the $J/\psi - \psi'$ channel, i.e., $s'_0 < m_\psi^2$. Afterwards, we choose (M_1^2, \mathbf{s}_0) in accordance with Eq. (11), but do not modify (M_2^2, s'_0) . By this way, we include into consideration $g_1^*(q^2)$ and obtain the equation containing $g_1(q^2)$ and $g_1^*(q^2)$. This means that remaining terms in Eq. (19) are included in ‘‘higher resonances and continuum states’’ and their effects

are implicitly taken into account in $\Pi(M^2, s_0, q^2)$ through the quark-hadron duality. Then, using results for $g_1(q^2)$, we calculate the form factor $g_1^*(q^2)$ that determines the width of the process $X_{4c}^* \rightarrow J/\psi J/\psi$.

At the new stage of studies, we consider the equation for the form factors $g_1(q^2)$ and $g_2(q^2)$. The latter corresponds to the vertex $X_{4c} J/\psi \psi'$, and formally describes the channel $X_{4c} \rightarrow J/\psi \psi'$. This decay mode of X_{4c} is kinematically forbidden, because the threshold 6737 MeV for production of the $J/\psi \psi'$ pair exceeds the mass of the tetraquark X_{4c} . But $g_2(q^2)$ is required to determine the form factor $g_2^*(q^2)$ of interest. To extract $g_2(q^2)$, we fix (M_1^2, s_0) by means of Eq. (8), but choose (M_2^2, s_0^*) in the form

$$M_2^2 \in [4, 5] \text{ GeV}^2, \quad s_0^{*'} \in [15, 16] \text{ GeV}^2, \quad (23)$$

where $s_0^{*'} < m_{\psi(3S)}^2$. Finally, using for the $X_{4c} - X_{4c}^*$ and $J/\psi - \psi'$ channels Eqs. (11) and (23), we calculate the last form factor $g_2^*(q^2)$.

The SR method allows one to calculate the form factors in the deep-Euclidean region $q^2 < 0$. All functions $g_i^{(*)}(q^2)$ in the present work are calculated in the region $q^2 = -(1 - 10) \text{ GeV}^2$. But partial widths of the decays under consideration are determined by values of these form factors at the mass shell $q^2 = m_J^2$. To solve this problem, we introduce a new variable $Q^2 = -q^2$ and denote the obtained functions by $g_i^{(*)}(Q^2)$. Afterwards, we use a fit functions $\mathcal{G}_i^{(*)}(Q^2)$ that at momenta $Q^2 > 0$ are equal to the SR's results, but can be extrapolated to the domain of $Q^2 < 0$. In present article, we use functions $\mathcal{G}_i(Q^2)$

$$\mathcal{G}_i(Q^2) = \mathcal{G}_i^0 \exp \left[c_i^1 \frac{Q^2}{m^2} + c_i^2 \left(\frac{Q^2}{m^2} \right)^2 \right], \quad (24)$$

with parameters \mathcal{G}_i^0 , c_i^1 and c_i^2 . It is worth noting that in the case of $g_1^*(q^2)$ and $g_2^*(q^2)$ the parameter m in Eq. (24) is the mass of the tetraquark X_{4c}^* , whereas for the intermediate functions $g_1(q^2)$ and $g_2(q^2)$, we use the mass m_0 of X_{4c} .

Results obtained for $g_1^*(q^2)$ and $g_2^*(q^2)$ are plotted in Fig. 2. Computations demonstrate that $\mathcal{G}_1^{0*} = 0.68 \text{ GeV}^{-1}$, $c_1^{1*} = 3.93$, and $c_1^{2*} = -4.33$ lead to nice agreement with the sum rule's data for $g_1^*(Q^2)$. At the mass shell $q^2 = m_J^2$ the function $\mathcal{G}_1^*(Q^2)$ is equal to

$$g_1^* \equiv \mathcal{G}_1^*(-m_J^2) = (3.1 \pm 0.5) \times 10^{-1} \text{ GeV}^{-1}. \quad (25)$$

The width of the decay $X_{4c}^* \rightarrow J/\psi J/\psi$ can be obtained by employing the expression

$$\Gamma[X_{4c}^* \rightarrow J/\psi J/\psi] = g_1^{*2} \frac{\lambda_1}{8\pi} \left(\frac{m_J^4}{m^2} + \frac{2\lambda_1^2}{3} \right), \quad (26)$$

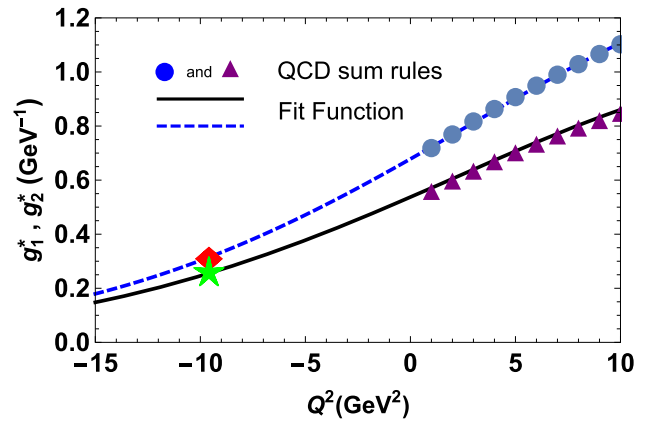


Fig. 2 The QCD results and fit functions for the form factors $g_1^*(Q^2)$ (dashed curve) and $g_2^*(Q^2)$ (solid curve). The red diamond and green star denote the point $Q^2 = -m_J^2$, where the strong couplings g_1^* and g_2^* are evaluated

where $\lambda_1 = \lambda(m, m_J, m_J)$ and

$$\lambda(m_1, m_2, m_3) = \frac{[m_1^4 + m_2^4 + m_3^4 - 2(m_1^2 m_2^2 + m_1^2 m_3^2 + m_2^2 m_3^2)]^{1/2}}{2m_1}. \quad (27)$$

Then it is not difficult to find that

$$\Gamma[X_{4c}^* \rightarrow J/\psi J/\psi] = (30.1 \pm 8.3) \text{ MeV}. \quad (28)$$

In the case of $g_2^*(Q^2)$, similar investigations give for the parameters of the function $\mathcal{G}_2^*(Q^2)$ following results: $\mathcal{G}_2^{0*} = 0.54 \text{ GeV}^{-1}$, $c_2^{1*} = 3.28$, and $c_2^{2*} = -4.26$. The strong coupling g_2^* equals to

$$g_2^* \equiv \mathcal{G}_2^*(-m_J^2) = (2.5 \pm 0.5) \times 10^{-1} \text{ GeV}^{-1}. \quad (29)$$

Partial width of the process $X_{4c}^* \rightarrow J/\psi \psi'$ is given by the formula

$$\Gamma[X_{4c}^* \rightarrow J/\psi \psi'] = g_2^{*2} \frac{\lambda_2}{8\pi} \left(\frac{m_{\psi'}^2 m_J^2}{m^2} + \frac{2\lambda_2^2}{3} \right), \quad (30)$$

where $\lambda_2 = \lambda(m, m_{\psi'}, m_J)$. This leads to the prediction

$$\Gamma[X_{4c}^* \rightarrow J/\psi \psi'] = (11.5 \pm 3.3) \text{ MeV}. \quad (31)$$

The results obtained for these two decay channels are collected in Table 1.

The decays $X_{4c}^* \rightarrow \eta_c \eta_c$ and $X_{4c}^* \rightarrow \eta_c \eta_c(2S)$ can be explored in the context of this scheme as well. In this case, the double Borel transformation of the amplitude $\Pi_{\eta_c}^{\text{Phys}}(p^2, p'^2, q^2)$ equals to

$$\mathcal{B}\Pi_{\eta_c}^{\text{Phys}}(p^2, p'^2, q^2) = g_3(q^2) \frac{f_0 m_0 f_{\eta_c}^2 m_{\eta_c}^4}{4m_c^2} R(m_0, m_{\eta_c})$$

$$\begin{aligned}
 &+g_3^*(q^2)\frac{fmf_{\eta_c}^2m_{\eta_c}^4}{4m_c^2}R(m,m_{\eta_c})+g_4(q^2)\frac{f_0m_0f_{\eta_c}m_{\eta_c}^2}{4m_c^2} \\
 &\times f_{\eta_c(2S)}m_{\eta_c(2S)}^2R(m_0,m_{\eta_c(2S)})+g_4^*(q^2)\frac{fmf_{\eta_c}m_{\eta_c}^2}{4m_c^2} \\
 &\times f_{\eta_c(2S)}m_{\eta_c(2S)}^2R(m,m_{\eta_c(2S)})+\dots, \tag{32}
 \end{aligned}$$

where $m_{\eta_c} = (2983.9 \pm 0.4)$ MeV, $f_{\eta_c} = (398.1 \pm 1.0)$ MeV and $m_{\eta_c(2S)} = (3637.5 \pm 1.1)$ MeV, $f_{\eta_c(2S)} = 331$ MeV are the spectroscopic parameters of the η_c and $\eta_c(2S)$ mesons [27,29]. The function $R(a,b)$ is defined by the formula

$$R(a,b) = \frac{(a^2 + b^2 - q^2)}{2(q^2 - m_{\eta_c}^2)} e^{-a^2/M_1^2} e^{-b^2/M_2^2}. \tag{33}$$

The invariant amplitude $\Pi_{\eta_c}^{\text{OPE}}(p^2, p'^2, q^2)$ was calculated in our article [19]. Here, one should take into account that the regions (M_2^2, s'_0) and (M_2^2, s_0') for $\eta_c - \eta_c(2S)$ channel are given by the expressions

$$M_2^2 \in [3.5, 4.5] \text{ GeV}^2, \quad s'_0 \in [11, 12] \text{ GeV}^2, \tag{34}$$

and

$$M_2^2 \in [3.5, 4.5] \text{ GeV}^2, \quad s_0' \in [13, 14] \text{ GeV}^2, \tag{35}$$

respectively. In the case of $g_3^*(Q^2)$, our studies lead for the parameters of the function $\mathcal{G}_3^*(Q^2)$ to predictions: $\mathcal{G}_3^{0*} = 0.39 \text{ GeV}^{-1}$, $c_3^{1*} = 4.01$, and $c_3^{2*} = -4.99$. Then the coupling g_3^* is equal to

$$g_3^* \equiv \mathcal{G}_3^*(-m_{\eta_c}^2) = (1.7 \pm 0.4) \times 10^{-1} \text{ GeV}^{-1}. \tag{36}$$

The width of the decay $X_{4c}^* \rightarrow \eta_c \eta_c$ can be found by means of the formula

$$\Gamma[X_{4c}^* \rightarrow \eta_c \eta_c] = g_3^{*2} \frac{m_{\eta_c}^2 \lambda_3}{8\pi} \left(1 + \frac{\lambda_3^2}{m_{\eta_c}^2} \right), \tag{37}$$

where $\lambda_3 = \lambda(m, m_{\eta_c}, m_{\eta_c})$. Numerical computations yield

$$\Gamma[X_{4c}^* \rightarrow \eta_c \eta_c] = (30.6 \pm 10.5) \text{ MeV}. \tag{38}$$

For the second decay $X_{4c}^* \rightarrow \eta_c \eta_c(2S)$, we get

$$\begin{aligned}
 g_4^* &\equiv \mathcal{G}_4^*(-m_{\eta_c}^2) = (1.4 \pm 0.3) \times 10^{-1} \text{ GeV}^{-1}, \\
 \Gamma[X_{4c}^* \rightarrow \eta_c \eta_c(2S)] &= (16.6 \pm 5.5) \text{ MeV}, \tag{39}
 \end{aligned}$$

where $\mathcal{G}_4^*(Q^2)$ is the function with parameters $\mathcal{G}_4^{0*} = 0.32 \text{ GeV}^{-1}$, $c_4^{1*} = 4.06$, and $c_4^{2*} = -5.02$.

Treatment of the channels $X_{4c}^* \rightarrow \eta_c \chi_{c1}$, $\chi_{c0} \chi_{c0}$, and $\chi_{c1} \chi_{c1}$ is done by taking into account vertices of the tetraquarks X_{4c} and X_{4c}^* with these meson pairs. Therefore, the physical side of the sum rules consists of two terms. In the

case of the $\eta_c \chi_{c1}$ mesons, both the ground-level tetraquark X_{4c} and its excited state X_{4c}^* decays to this meson pair. Therefore, to find the partial decay width of the process $X_{4c}^* \rightarrow \eta_c \chi_{c1}$, we use the form factor $g_5(q^2)$ studied in Ref. [19], and extract $g_5^*(q^2)$ necessary to compute the coupling g_5^* at the mass shell $q^2 = m_{\eta_c}^2$. The corresponding fit function $\mathcal{G}_5^*(Q^2)$ has the parameters: $\mathcal{G}_5^{0*} = 3.46$, $c_5^{1*} = 3.59$, and $c_5^{2*} = -4.72$.

The remaining processes $X_{4c}^* \rightarrow \chi_{c0} \chi_{c0}$ and $\chi_{c1} \chi_{c1}$ are investigated by the same manner, the difference being that decays of X_{4c} to mesons $\chi_{c0} \chi_{c0}$, and $\chi_{c1} \chi_{c1}$ are not kinematically allowed channels, but we compute relevant form factors to find strong couplings g_6^* and g_7^* of interests. The related correlation functions are calculated in the present work for the first time and given by the expressions (A.3) and (A.4). The final results of analysis are collected in Table 1. Let us note only that in numerical computations, we employ the SR predictions for the decay constants $f_{\chi_{c1}} = (344 \pm 27)$ MeV and $f_{\chi_{c0}} = 343$ MeV [30,31].

Having used results for the partial widths of the excited X_{4c}^* tetraquark's decay channels, we estimate its full width

$$\Gamma = (144 \pm 18) \text{ MeV}. \tag{40}$$

3 Hadronic molecule $\chi_{c1} \chi_{c1}$

Here, we investigate the hadronic molecule $\mathcal{M} = \chi_{c1} \chi_{c1}$ and calculate the mass and current coupling of this structure, which will be used to determine its kinematically allowed decay channels. Decays of the molecule \mathcal{M} and its full width are also studied in this section.

3.1 Mass and current coupling

The sum rules for the mass \tilde{m} and current coupling \tilde{f} of the molecule \mathcal{M} can be extracted by exploring the correlation function

$$\Pi(p) = i \int d^4x e^{ipx} \langle 0 | \mathcal{T} \{ \tilde{J}(x) \tilde{J}^\dagger(0) \} | 0 \rangle. \tag{41}$$

Here, $\tilde{J}(x)$ is the interpolating current for \mathcal{M}

$$\tilde{J}(x) = \bar{c}_a(x) \gamma_5 \gamma_\mu c_a(x) \bar{c}_b(x) \gamma_5 \gamma^\mu c_b(x), \tag{42}$$

with a , and b being the color indices. We are going to calculate spectroscopic parameters of the ground-level molecule \mathcal{M} , therefore the physical side of the SRs is given by only one term

$$\Pi^{\text{Phys}}(p) = \frac{\tilde{f}^2 \tilde{m}^2}{\tilde{m}^2 - p^2} + \dots \tag{43}$$

Table 1 Decay channels of the tetraquark X_{4c}^* and hadronic molecule \mathcal{M} , strong couplings g_i^* and $G_i^{(*)}$, and partial widths Γ_i and $\tilde{\Gamma}_i$. The couplings g_5^* and G_5 are dimensionless. For all decays of the tetraquark X_{4c}^* the parameters M_1^2 and s_0^* vary in the regions [5.5, 7] GeV^2 and

[55, 56] GeV^2 , respectively. In the case of the molecule \mathcal{M} the parameters are $M_1^2 \in [6, 8] \text{GeV}^2$ and $s_0 \in [63, 65] \text{GeV}^2$ for all considered processes

i	Channels	$M_2^2(\text{GeV}^2)$	$s_0^{(*)'}(\text{GeV}^2)$	$g_i^* \times 10 (\text{GeV}^{-1})$	$\Gamma_i(\text{MeV})$	$G_i^{(*)} \times 10 (\text{GeV}^{-1})$	$\tilde{\Gamma}_i(\text{MeV})$
1	$J/\psi J/\psi$	4–5	12–13	3.1 ± 0.5	30.1 ± 8.3	3.5 ± 0.7	36.1 ± 10.5
2	$J/\psi \psi'$	4–5	15–16	2.5 ± 0.5	11.5 ± 3.3	3.2 ± 0.5	16.2 ± 5.1
3	$\eta_c \eta_c$	3.5–4.5	11–12	1.7 ± 0.4	30.6 ± 10.5	2.0 ± 0.4	42.3 ± 12.2
4	$\eta_c \eta_c(2S)$	3.5–4.5	13–14	1.4 ± 0.3	16.6 ± 5.5	1.3 ± 0.3	14.7 ± 5.1
5	$\eta_c \chi_{c1}$	4–5	13–14	16.4 ± 3.8	11.6 ± 4.1	18.3 ± 4.1	12.8 ± 4.2
6	$\chi_{c0} \chi_{c0}$	4–5	14–14.9	2.1 ± 0.4	28.8 ± 7.9	2.3 ± 0.5	29.9 ± 9.4
7	$\chi_{c1} \chi_{c1}$	4–5	13–14	3.5 ± 0.5	14.4 ± 4.2	4.1 ± 0.8	16.5 ± 4.7

It is calculated by taking into account the matrix element

$$\langle 0 | \tilde{J} | \mathcal{M} \rangle = \tilde{f} \tilde{m}. \tag{44}$$

The invariant amplitude that is required for following analysis is $\Pi^{\text{Phys}}(p^2) = \tilde{f}^2 \tilde{m}^2 / (\tilde{m}^2 - p^2)$.

The correlation function $\Pi^{\text{OPE}}(p)$ in terms of the c -quark propagators is determined by Eq. (45)

$$\begin{aligned} \Pi^{\text{OPE}}(p) = & i \int d^4x e^{ipx} \left\{ \text{Tr} \left[\gamma_5 \gamma_\mu S_c^{ba'}(x) \gamma_\nu \gamma_5 S_c^{a'b}(-x) \right] \right. \\ & \times \text{Tr} \left[\gamma_5 \gamma^\mu S_c^{ab'}(x) \gamma^\nu \gamma_5 S_c^{b'a}(-x) \right] - \text{Tr} \left[\gamma_5 \gamma_\mu S_c^{bb'}(x) \gamma_\nu \right. \\ & \times \gamma_5 S_c^{b'a}(-x) \gamma_5 \gamma^\mu S_c^{aa'}(x) \gamma^\nu \gamma_5 S_c^{a'b}(-x) \left. \right] - \text{Tr} \left[\gamma_5 \gamma_\mu \right. \\ & \times S_c^{ba'}(x) \gamma_\nu \gamma_5 S_c^{a'a}(-x) \gamma_5 \gamma^\mu S_c^{ab'}(x) \gamma^\nu \gamma_5 S_c^{b'b}(-x) \left. \right] \\ & + \text{Tr} \left[\gamma_5 \gamma_\mu S_c^{bb'}(x) \gamma_\nu \gamma_5 S_c^{b'b}(-x) \right] \text{Tr} \left[\gamma_5 \gamma^\mu S_c^{aa'}(x) \gamma^\nu \right. \\ & \left. \times \gamma_5 S_c^{a'a}(-x) \right] \left. \right\}. \tag{45} \end{aligned}$$

It is convenient to denote the invariant amplitude of the QCD side by $\Pi^{\text{OPE}}(p^2)$. Then, the sum rules for the mass and current coupling take simple forms

$$\tilde{m}^2 = \frac{\Pi'(M^2, s_0)}{\Pi(M^2, s_0)} \tag{46}$$

and

$$\tilde{f}^2 = \frac{e^{\tilde{m}^2/M^2}}{\tilde{m}^2} \Pi(M^2, s_0), \tag{47}$$

where $\Pi'(M^2, s_0) = d\Pi(M^2, s_0)/d(-1/M^2)$. Here, $\Pi(M^2, s_0)$ is the amplitude $\Pi^{\text{OPE}}(p^2)$ obtained after the Borel transformation and continuum subtraction operations.

Computations lead to the following constraints on the parameters M^2 and s_0

$$M^2 \in [6, 8] \text{GeV}^2, s_0 \in [63, 65] \text{GeV}^2. \tag{48}$$

It is not difficult to check that PC meets usual requirements of SR computations. In Fig. 3, we plot dependence of the pole contribution on the Borel parameter. It is seen, that expect for a small region, PC is larger than 0.5. On average in s_0 the PC exceeds 0.5 for all values of M^2 .

The mass and current coupling of the molecule \mathcal{M} are

$$\begin{aligned} \tilde{m} &= (7180 \pm 120) \text{MeV}, \\ \tilde{f} &= (1.06 \pm 0.13) \times 10^{-1} \text{GeV}^4, \end{aligned} \tag{49}$$

respectively. It is worth to note that \tilde{m} and \tilde{f} in Eq. (49) are mean values of the mass and current coupling averaged over the working regions (48). It overshoots the mass 7022 MeV of two χ_{c1} mesons by 160 MeV and is unstable against decays to these particles.

In Fig. 4, we plot the mass \tilde{m} as a function of M^2 and s_0 , in which its residual dependence on these parameters is clear. It is also useful to estimate a gap between the ground-state \mathcal{M} and excited molecules \mathcal{M}^* . The mass \tilde{m}^* of the state \mathcal{M}^* should obey the constraint $\tilde{m}^* \geq \sqrt{s_0}$, i.e., $\tilde{m}^* \geq 8 \text{GeV}$, which implies an approximately 800 MeV mass splitting between these molecules.

3.2 Width of \mathcal{M}

Decay channels of the hadronic molecule \mathcal{M} do not differ from that of the tetraquark X_{4c}^* . A difference appears in treatment of these processes. Indeed, the molecule \mathcal{M} is ground-state particle in its class, therefore physical side of relevant sum rules in \mathcal{M} channel contains terms connected only with its decays.

Because the resonances under investigation were detected in the di- J/ψ and $J/\psi \psi'$ mass distributions, we concentrate on the decays $\mathcal{M} \rightarrow J/\psi J/\psi$ and $\mathcal{M} \rightarrow J/\psi \psi'$. The correlation function required for this analysis is given by the formula

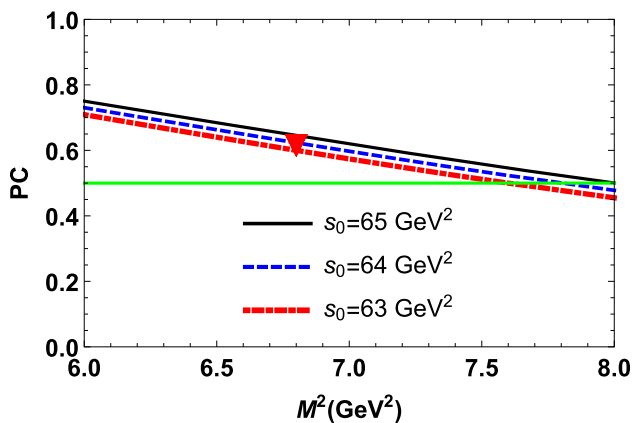
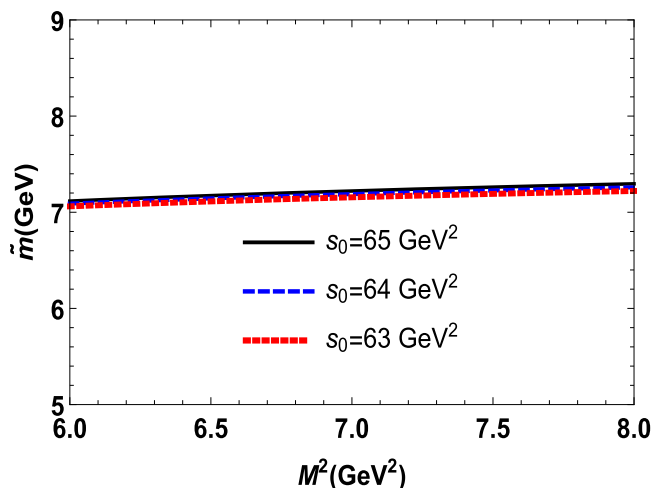


Fig. 3 Dependence of PC on the Borel parameter M^2 . The horizontal line shows the border $PC = 0.5$. The red triangle fix the position, where the mass of the molecule $\chi_{c1}\chi_{c1}$ has been evaluated

$$\begin{aligned} &\tilde{\Pi}_{\mu\nu}(p, p') \\ &= i^2 \int d^4x d^4y e^{ip'y} e^{-ipx} \langle 0 | T \{ J_\mu^\psi(y) \\ &\quad \times J_\nu^\psi(0) \tilde{J}^\dagger(x) \} | 0 \rangle. \end{aligned} \tag{50}$$

As usual, we express $\tilde{\Pi}_{\mu\nu}(p, p')$ in terms of the physical parameters of particles involved in the decay process. To this end, we write it in the following form

$$\begin{aligned} \tilde{\Pi}_{\mu\nu}^{\text{Phys}}(p, p') &= \frac{\langle 0 | J_\mu^\psi | J/\psi(p') \rangle \langle 0 | J_\nu^\psi | J/\psi(q) \rangle}{p'^2 - m_J^2} \frac{\langle 0 | J_\nu^\psi | J/\psi(q) \rangle}{q^2 - m_J^2} \\ &\times \langle J/\psi(p') J/\psi(q) | \mathcal{M}(p) \rangle \frac{\langle \mathcal{M}(p) | \tilde{J}^\dagger | 0 \rangle}{p^2 - \tilde{m}^2} \\ &+ \frac{\langle 0 | J_\mu^\psi | \psi(p') \rangle \langle 0 | J_\nu^\psi | J/\psi(q) \rangle}{p'^2 - m_\psi^2} \frac{\langle 0 | J_\nu^\psi | J/\psi(q) \rangle}{q^2 - m_J^2} \\ &\times \langle \psi(p') J/\psi(q) | \mathcal{M}(p) \rangle \frac{\langle \mathcal{M}(p) | \tilde{J}^\dagger | 0 \rangle}{p^2 - \tilde{m}^2} + \dots \end{aligned} \tag{51}$$



We have already defined the matrix elements of the hadronic molecule \mathcal{M} and mesons J/ψ and ψ' . The vertices $\mathcal{M}J/\psi$ and $\mathcal{M}J/\psi\psi'$ after some substitutions are given by Eq. (16). As in previous section, we use the amplitude $\tilde{\Pi}^{\text{Phys}}(p^2, p'^2, q^2)$ which in $\tilde{\Pi}_{\mu\nu}^{\text{Phys}}(p, p')$ corresponds to a term proportional to $g_{\mu\nu}$. The double Borel transformation of the function $\tilde{\Pi}^{\text{Phys}}(p^2, p'^2, q^2)$ over the variables $-p^2$ and $-p'^2$ is equal to

$$\begin{aligned} \mathcal{B}\tilde{\Pi}^{\text{Phys}}(p^2, p'^2, q^2) &= G_1(q^2) \tilde{f}\tilde{m} f_J^2 m_J^2 F(\tilde{m}, m_J) \\ &+ G_1^*(q^2) \tilde{f}\tilde{m} f_J m_J f_\psi m_\psi F(\tilde{m}, m_\psi) + \dots \end{aligned} \tag{52}$$

The correlation function $\tilde{\Pi}_{\mu\nu}^{\text{OPE}}(p, p')$ is given by the formula

$$\begin{aligned} \tilde{\Pi}_{\mu\nu}^{\text{OPE}}(p, p') &= 2i^2 \int d^4x d^4y e^{-ipx} e^{ip'y} \left\{ \text{Tr} \left[\gamma_\nu S_c^{jb}(-x) \right. \right. \\ &\quad \times \gamma^\alpha \gamma_5 S_c^{bj}(x) \left. \right] \text{Tr} \left[\gamma_\mu S_c^{ia}(y-x) \gamma_\alpha \gamma_5 S_c^{ai}(x-y) \right] \\ &\quad - \text{Tr} \left[\gamma_\mu S_c^{ia}(y-x) \gamma_\alpha \gamma_5 S_c^{aj}(x) \gamma_\nu S_c^{jb}(-x) \gamma^\alpha \right. \\ &\quad \left. \times \gamma_5 S_c^{bi}(x-y) \right] \left. \right\}. \end{aligned} \tag{53}$$

The QCD side of the sum rule and amplitude $\tilde{\Pi}^{\text{OPE}}(p^2, p'^2, q^2)$ are extracted from this expression. The strategy pursued in our study of these processes repeats one used in Sect. 2 while considering decays of the tetraquark X_{4c}^* . We first determine the form factor $G_1(q^2)$ utilizing the “ground-state + continuum” scheme. The parameters (M_1^2, s_0) are universal for all decays of \mathcal{M} and are presented in Eq. (48). The second pair of the parameters (M_2^2, s_0') corresponding to $J/\psi J/\psi$ decay can be found in Eq. (22). Once determined $G_1(q^2)$, in the second stage of computations we choose (M_2^2, s_0^*) from Eq. (23) and employ information on $G_1(q^2)$ to find the form factor $G_1^*(q^2)$, responsible for the process $\mathcal{M} \rightarrow J/\psi\psi'$. The functions $\mathcal{G}_8(Q^2)$ and $\mathcal{G}_8^*(Q^2)$ are formed by the parameters

$$\mathcal{G}_8^0 = 0.76 \text{ GeV}^{-1} \quad c_8^1 = 3.32, \quad c_8^2 = -4.19,$$

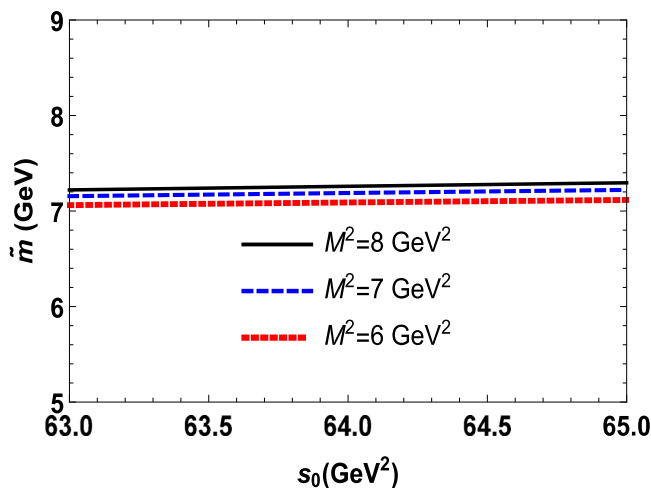


Fig. 4 Mass \tilde{m} of the molecule $\chi_{c1}\chi_{c1}$

$$G_8^{0*} = 0.68 \text{ GeV}^{-1}, c_8^{1*} = 3.20, c_8^{2*} = -4.11. \tag{54}$$

The strong couplings G_1 and G_1^* are extracted from these functions at the mass shells $Q^2 = -m_J^2$.

This approach is also valid for the channels $\mathcal{M} \rightarrow \eta_c \eta_c$ and $\mathcal{M} \rightarrow \eta_c \eta_c(2S)$. The correlation function required for these decays is written down below

$$\begin{aligned} \Pi^{\text{OPE}}(p, p') = & 2 \int d^4x d^4y e^{-ipx} e^{ip'y} \left\{ \text{Tr} \left[\gamma_5 S_c^{ia}(y-x) \right. \right. \\ & \times \gamma_\alpha \gamma_5 S_c^{ai}(x-y) \left. \right] \text{Tr} \left[\gamma_5 S_c^{jb}(-x) \gamma^\alpha \gamma_5 S_c^{bj}(x) \right] \\ & - \text{Tr} \left[\gamma_5 S_c^{ia}(y-x) \gamma_\alpha \gamma_5 S_c^{aj}(x) \gamma_5 S_c^{jb}(-x) \gamma^\alpha \right. \\ & \left. \left. \times \gamma_5 S_c^{bi}(x-y) \right] \right\}. \tag{55} \end{aligned}$$

The functions $G_9(Q^2)$ and $G_9^*(Q^2)$ needed to extrapolate the form factors $G_2(q^2)$ and $G_2^*(q^2)$ are determined by the parameters: $G_9^0 = 0.46 \text{ GeV}^{-1}$, $c_9^1 = 3.93$, $c_9^2 = -4.83$ and $G_9^{0*} = 0.30 \text{ GeV}^{-1}$, $c_9^{1*} = 3.90$, $c_9^{2*} = -4.81$. These functions at the mass shells $Q^2 = -m_J^2$ fix the couplings G_2 and G_2^* , respectively.

The decays $\mathcal{M} \rightarrow \eta_c \chi_{c1}$, $\chi_{c0} \chi_{c0}$, and $\chi_{c1} \chi_{c1}$ are investigated directly in the context of the ‘‘ground-state + continuum’’ approach. Corresponding functions $\Pi_\mu^{\text{OPE}}(p, p')$, $\Pi^{\text{OPE}}(p, p')$ and $\widehat{\Pi}_{\mu\nu}^{\text{OPE}}(p, p')$ can found in Appendix as Eqs. (A.5)–(A.7). Predictions obtained for the partial widths of different modes of the hadronic molecule \mathcal{M} , strong couplings and related parameters are presented in Table 1. It should be noted that, to collect results obtained in this work in the framework of a single Table, the couplings G_1^* , G_2 and G_2^* are placed there under numbers G_2^* , G_3 and G_4^* , respectively.

For the full width of the hadronic molecule, we get

$$\widetilde{\Gamma} = (169 \pm 21) \text{ MeV}, \tag{56}$$

which characterizes it as a wide structure.

4 Summing up

In the present work, we have explored radially excited tetraquark X_{4c}^* and hadronic molecule $\mathcal{M} = \chi_{c1} \chi_{c1}$. We have computed their masses and full widths using the QCD sum rule method and interpolating currents $J(x)$ and $\widetilde{J}(x)$. Obtained results have been confronted with available data of the ATLAS-CMS Collaborations on the heaviest resonance $X(7300)$.

The LHCb fixed this state at 7.2 GeV, but did not provide other information. The CMS measured parameters of this resonance and found that

$$m^{\text{CMS}} = 7287_{-18}^{+20} \pm 5 \text{ MeV},$$

$$\Gamma^{\text{CMS}} = 95_{-40}^{+59} \pm 19 \text{ MeV}. \tag{57}$$

The ATLAS Collaboration observed $X(7300)$ in the $J/\psi \psi'$ mass distribution and also reported the mass and width of this state

$$\begin{aligned} m^{\text{ATL}} &= 7220 \pm 30_{-30}^{+20} \text{ MeV}, \\ \Gamma^{\text{ATL}} &= 100_{-70-50}^{+130+60} \text{ MeV}. \tag{58} \end{aligned}$$

As is seen, experimental data suffer from big errors: only in the case of Eq. (57) they are relatively small.

Comparing our findings $m = (7235 \pm 75) \text{ MeV}$ and $\widetilde{m} = (7180 \pm 120) \text{ MeV}$ with corresponding experimental data and taking into account errors of calculations and measurements, we conclude that masses of the excited tetraquark X_{4c}^* and hadronic molecule \mathcal{M} are compatible with m^{CMS} and m^{ATL} . In other words, at this phase of analysis, it is difficult to make assignment for the resonance $X(7300)$.

The full widths of the structures X_{4c}^* and \mathcal{M} provide very important information for this purpose. It is interesting that $X(7300)$ is narrowest fully charmed state detected by the ATLAS and CMS experiments provided one ignores errors of measurements. The four-quark structures X_{4c}^* and \mathcal{M} have the widths $\Gamma = (144 \pm 18) \text{ MeV}$ and $\widetilde{\Gamma} = (169 \pm 21) \text{ MeV}$, respectively. As is seen, within uncertainties of theoretical analysis they agree with results of measurements. Because masses of these structures are also consistent with existing data, both the excited tetraquark X_{4c}^* and hadronic molecule \mathcal{M} may be considered as natural candidates to the observed state $X(7300)$.

For more strong conclusions about internal organization of $X(7300)$, it is useful to examine an overlap of the currents $J(x)$ and $\widetilde{J}(x)$ with the physical state $X(7300)$ modeled as the structures X_{4c}^* or \mathcal{M} . This information is encoded in the matrix element

$$\langle 0 | J | X(7300) \rangle = \Lambda_J. \tag{59}$$

By employing Eqs. (10) and (49) obtained for the diquark-antidiquark and molecule currents, we find that the matrix element in Eq. (59) equals to $\Lambda_J \approx 0.58 \text{ GeV}^5$ and $\Lambda_{\widetilde{J}} \approx 0.76 \text{ GeV}^5$, respectively. This means, that the fully charmed resonance $X(7300)$ couples with a larger strength to $\chi_{c1} \chi_{c1}$ molecule current than to the current from Eq. (2). But from the ratio $\Lambda_J / \Lambda_{\widetilde{J}} \approx 0.76$ it also becomes clear that $X(7300)$ can not be interpreted as a pure molecule state. Indeed, the diquark-antidiquark current $J(x)$ through Fierz transformations can be expressed as a weighted sum of $\widetilde{J}(x)$ and other currents. Then if $X(7300)$ had a pure molecule structure, the ratio $\Lambda_J / \Lambda_{\widetilde{J}}$ would be equal to a weight of the molecule component in $J(x)$, and considerably smaller than 0.76 [24]. Because this is not a case, we can conclude that $X(7300)$ contains a sizeable X_{4c}^* component. As a result, a preferable

model for the resonance $X(7300)$ is the admixture of the molecule \mathcal{M} with considerable piece of the tetraquark X_{4c}^* .

Parameters of such mixing depend on precision of the mass and width of the resonance $X(7300)$ measured by experimental groups. Accuracy of the theoretical results are also important. In the sum rule method physical observables are evaluated with some accuracy and contain uncertainties which can be kept under control. The ambiguities in the masses and widths of the structures X_{4c}^* and \mathcal{M} are typical for such kind of investigations, and can hardly be reduced. Therefore, for quantitative analysis of the $\mathcal{M}-X_{4c}^*$ mixing phenomenon one needs more precise experimental data. This is true not only for $X(7300)$, but also for other fully charmed X resonances.

Data Availability Statement This manuscript has no associated data or the data will not be deposited. [Authors' comment: All the numerical and mathematical data have been included in the paper and we have no other data regarding this paper].

Open Access This article is licensed under a Creative Commons Attribution 4.0 International License, which permits use, sharing, adaptation, distribution and reproduction in any medium or format, as long as you give appropriate credit to the original author(s) and the source, provide a link to the Creative Commons licence, and indicate if changes were made. The images or other third party material in this article are included in the article's Creative Commons licence, unless indicated otherwise in a credit line to the material. If material is not included in the article's Creative Commons licence and your intended use is not permitted by statutory regulation or exceeds the permitted use, you will need to obtain permission directly from the copyright holder. To view a copy of this licence, visit <http://creativecommons.org/licenses/by/4.0/>.
 Funded by SCOAP³. SCOAP³ supports the goals of the International Year of Basic Sciences for Sustainable Development.

Appendix: Heavy quark propagator and different correlation functions

In the present paper, for the heavy quark propagator $S_Q^{ab}(x)$ ($Q = c, b$), we employ the following expression

$$S_Q^{ab}(x) = i \int \frac{d^4k}{(2\pi)^4} e^{-ikx} \left\{ \frac{\delta_{ab}(\not{k} + m_Q)}{k^2 - m_Q^2} - \frac{g_s G_{ab}^{\alpha\beta} \sigma_{\alpha\beta}(\not{k} + m_Q) + (\not{k} + m_Q) \sigma_{\alpha\beta}}{4(k^2 - m_Q^2)^2} + \frac{g_s^2 G^2}{12} \delta_{ab} m_Q \frac{k^2 + m_Q \not{k}}{(k^2 - m_Q^2)^4} + \dots \right\}. \tag{A.1}$$

Here, we have introduced the notations

$$G_{ab}^{\alpha\beta} \equiv G_A^{\alpha\beta} \lambda_{ab}^A / 2, \quad G^2 = G_{\alpha\beta}^A G_A^{\alpha\beta}, \tag{A.2}$$

with $G_A^{\alpha\beta}$ being the gluon field-strength tensor, and λ^A -Gell-Mann matrices. The index A varies in the range $1 - 8$.

This Appendix also contains expressions of correlation functions, which are employed to calculate some of the strong couplings. In the case of the decay $X_{4c}^* \rightarrow \chi_{c0} \chi_{c0}$ the correlation function $\Pi^{\text{OPE}}(p, p')$ is given by the formula

$$\begin{aligned} \Pi^{\text{OPE}}(p, p') &= 2i^2 \int d^4x d^4y e^{-ipx} e^{ip'y} \\ &\times \left\{ \text{Tr} \left[S_c^{ia}(y-x) \gamma_\mu \tilde{S}_c^{jb}(-x) \tilde{S}_c^{bj}(x) \gamma^\mu S_c^{ai}(x-y) \right] \right. \\ &\left. - \text{Tr} \left[S_c^{ia}(y-x) \gamma_\mu \tilde{S}_c^{jb}(-x) \tilde{S}_c^{aj}(x) \gamma^\mu S_c^{bi}(x-y) \right] \right\}, \end{aligned} \tag{A.3}$$

where $\tilde{S}_c(x) = CS_c(x)C$, and C is the charge conjugation operator. The fit function $\mathcal{G}_6^*(Q^2)$ used to find the strong coupling g_6^* is fixed by the parameters $\mathcal{G}_6^{0*} = 0.51 \text{ GeV}^{-1}$, $c_6^{1*} = 3.11$, and $c_6^{2*} = -3.57$.

For the decay $X_{4c}^* \rightarrow \chi_{c1} \chi_{c1}$ the function $\Pi_{\mu\nu}^{\text{OPE}}(p, p')$ has the following form:

$$\begin{aligned} \Pi_{\mu\nu}^{\text{OPE}}(p, p') &= 2i^2 \int d^4x d^4y e^{-ipx} e^{ip'y} \\ &\times \left\{ \text{Tr} \left[\gamma_\mu \gamma_5 S_c^{ia}(y-x) \gamma_\alpha \tilde{S}_c^{jb}(-x) \gamma_5 \gamma_\nu \tilde{S}_c^{aj}(x) \gamma^\alpha S_c^{bi}(x-y) \right] \right. \\ &\left. - \text{Tr} \left[\gamma_\mu \gamma_5 S_c^{ia}(y-x) \gamma_\alpha \tilde{S}_c^{jb}(-x) \gamma_5 \gamma_\nu \tilde{S}_c^{bj}(x) \gamma^\alpha S_c^{ai}(x-y) \right] \right\}. \end{aligned} \tag{A.4}$$

In this case, the function $\mathcal{G}_7^*(Q^2)$ has the parameters: $\mathcal{G}_7^{0*} = 0.74 \text{ GeV}^{-1}$, $c_7^{1*} = 2.48$, and $c_7^{2*} = -3.01$.

The correlation functions for the decays of the hadronic molecule \mathcal{M} and functions to calculate the relevant strong couplings:

Decay $\mathcal{M} \rightarrow \eta_c \chi_{c1}$

$$\begin{aligned} \Pi_\mu^{\text{OPE}}(p, p') &= 2i^3 \int d^4x d^4y e^{-ipx} e^{ip'y} \\ &\times \left\{ \text{Tr} \left[\gamma_\mu \gamma_5 S_c^{ia}(y-x) \gamma_\alpha \gamma_5 S_c^{ai}(x-y) \right] \right. \\ &\times \text{Tr} \left[\gamma_5 S_c^{jb}(-x) \gamma^\alpha \gamma_5 S_c^{bj}(x) \right] \\ &- \text{Tr} \left[\gamma_\mu \gamma_5 S_c^{ia}(y-x) \gamma_\alpha \gamma_5 S_c^{aj}(x) \gamma_5 S_c^{jb} \right. \\ &\left. \times (-x) \gamma^\alpha \gamma_5 S_c^{bi}(x-y) \right] \left. \right\}, \end{aligned} \tag{A.5}$$

and the fit function $\mathcal{G}_{10}(Q^2)$ for $G_5(Q^2)$: $\mathcal{G}_{10}^0 = 3.85$, $c_{10}^1 = 3.51$, and $c_{10}^2 = -4.56$.

Decay $\mathcal{M} \rightarrow \chi_{c0} \chi_{c0}$

$$\begin{aligned} \Pi^{\text{OPE}}(p, p') &= -2i^2 \int d^4x d^4y e^{-ipx} e^{ip'y} \\ &\times \text{Tr} \left[S_c^{ia}(y-x) \gamma_\alpha \gamma_5 S_c^{aj}(x) S_c^{jb}(-x) \gamma^\alpha \gamma_5 S_c^{bi}(x-y) \right], \end{aligned}$$

(A.6)

and $G_6(Q^2)$: $G_{11}^0 = 0.55 \text{ GeV}^{-1}$, $c_{11}^1 = 3.06$, and $c_{11}^2 = -3.46$.

Decay $\mathcal{M} \rightarrow \chi_{c1} \chi_{c1}$

$$\begin{aligned} & \widehat{\Pi}_{\mu\nu}^{\text{OPE}}(p, p') \\ &= 2i^2 \int d^4x d^4y e^{-ipx} e^{ip'y} \\ & \times \left\{ \text{Tr} \left[\gamma_\mu \gamma_5 S_c^{ia}(y-x) \gamma_\alpha \gamma_5 S_c^{ai}(x-y) \right] \right. \\ & \times \text{Tr} \left[\gamma_\nu \gamma_5 S_c^{jb}(-x) \gamma^\alpha \gamma_5 S_c^{bj}(x) \right] \\ & \left. - \text{Tr} \left[\gamma_\mu \gamma_5 S_c^{ia}(y-x) \gamma_\alpha \gamma_5 S_c^{aj}(x) \gamma_\nu \gamma_5 S_c^{jb}(-x) \right] \right. \\ & \left. \times \gamma^\alpha \gamma_5 S_c^{bi}(x-y) \right\}, \end{aligned} \quad (\text{A.7})$$

and the parameters $G_{12}^0 = 0.86 \text{ GeV}^{-1}$, $c_{12}^1 = 2.41$, and $c_{12}^2 = -2.89$ to compute $G_7(Q^2)$.

References

- R. Aaij et al. (LHCb Collaboration), *Sci. Bull.* **65**, 1983 (2020)
- E. Bouhova-Thacker (ATLAS Collaboration), *PoS ICHEP2022*, 806 (2022)
- A. Hayrapetyan et al. (CMS Collaboration). [arXiv:2306.07164](https://arxiv.org/abs/2306.07164) [hep-ex]
- J.R. Zhang, *Phys. Rev. D* **103**, 014018 (2021)
- R.M. Albuquerque, S. Narison, A. Rabemananjara, D. Rabetiarivony, G. Randriamanatrika, *Phys. Rev. D* **102**, 094001 (2020)
- Z.G. Wang, *Nucl. Phys. B* **985**, 115983 (2022)
- W.C. Dong, Z.G. Wang, *Phys. Rev. D* **107**, 074010 (2023)
- R.N. Faustov, V.O. Galkin, E.M. Savchenko, *Symmetry* **14**, 2504 (2022)
- C. Becchi, A. Giachino, L. Maiani, E. Santopinto, *Phys. Lett. B* **806**, 135495 (2020)
- C. Becchi, A. Giachino, L. Maiani, E. Santopinto, *Phys. Lett. B* **811**, 135952 (2020)
- X.K. Dong, V. Baru, F.K. Guo, C. Hanhart, A. Nefediev, *Phys. Rev. Lett.* **126**, 132001 (2021). [erratum: *Phys. Rev. Lett.* **127**, 119901 (2021)]
- X.K. Dong, V. Baru, F.K. Guo, C. Hanhart, A. Nefediev, B.S. Zou, *Sci. Bull.* **66**, 2462 (2021)
- Z.R. Liang, X.Y. Wu, D.L. Yao, *Phys. Rev. D* **104**, 034034 (2021)
- P. Niu, Z. Zhang, Q. Wang, M.L. Du, *Sci. Bull.* **68**, 800 (2023)
- G.L. Yu, Z.Y. Li, Z.G. Wang, J. Lu, M. Yan, *Eur. Phys. J. C* **83**, 416 (2023)
- S.Q. Kuang, Q. Zhou, D. Guo, Q.H. Yang, L.Y. Dai, *Eur. Phys. J. C* **83**, 383 (2023)
- F. Feng, Y. Huang, Y. Jia, W.L. Sang, D.S. Yang, J.Y. Zhang, *Phys. Rev. D* **108**, L051501 (2023)
- L.M. Abreu, F. Carvalho, J.V.C. Cerquera, V.P. Goncalves. [arXiv:2306.12731](https://arxiv.org/abs/2306.12731) [hep-ph]
- S.S. Agaev, K. Azizi, B. Barsbay, H. Sundu, *Phys. Lett. B* **844**, 138089 (2023)
- S.S. Agaev, K. Azizi, B. Barsbay, H. Sundu, *Nucl. Phys. A* **1041**, 122768 (2024)
- S.S. Agaev, K. Azizi, B. Barsbay, H. Sundu, *Eur. Phys. J. Plus* **138**, 935 (2023)
- M.A. Shifman, A.I. Vainshtein, V.I. Zakharov, *Nucl. Phys. B* **147**, 385 (1979)
- M.A. Shifman, A.I. Vainshtein, V.I. Zakharov, *Nucl. Phys. B* **147**, 448 (1979)
- M. Nielsen, F.S. Navarra, S.H. Lee, *Phys. Rep.* **497**, 41 (2010)
- R.M. Albuquerque, J.M. Dias, K.P. Khemchandani, A. Martinez-Torres, F.S. Navarra, M. Nielsen, C.M. Zanetti, *J. Phys. G* **46**, 093002 (2019)
- S.S. Agaev, K. Azizi, H. Sundu, *Turk. J. Phys.* **44**, 95 (2020)
- R.L. Workman et al. [Particle Data Group], *Prog. Theor. Exp. Phys.* **2022**, 083C01 (2022)
- V.V. Kiselev, A.K. Likhoded, O.N. Pakhomova, V.A. Saleev, *Phys. Rev. D* **65**, 034013 (2002)
- D. Hatton et al. (HPQCD Collaboration), *Phys. Rev. D* **102**, 054511 (2020)
- E. Veli Veliev, K. Azizi, H. Sundu, G. Kaya, *PoS (Confinement X)* **339** (2012). [arXiv:1205.5703](https://arxiv.org/abs/1205.5703)
- E.V. Veliev, H. Sundu, K. Azizi, M. Bayar, *Phys. Rev. D* **82**, 056012 (2010)